*Proc. Natl. Acad. Sci. USA*
Vol. 93, pp. 5258–5263, May 1996
Biophysics

# Ultraviolet-B photodestruction of a light-harvesting complex

KAIQIN LAO AND ALEXANDER N. GLAZER*

Department of Molecular and Cell Biology, University of California, 229 Stanley Hall, MC 3206, Berkeley, CA 94720-3206

*Communicated by Howard K. Schachman, University of California, Berkeley, CA, February 2, 1996 (received for review November 28, 1995)*

ABSTRACT **Cyanobacteria are important contributors to global photosynthesis in both marine and terrestrial environments. Quantitative data are presented on UV-B-induced damage to the major cyanobacterial photosynthetic light harvesting complex, the phycobilisome, and to each of its constituent phycobiliproteins. The photodestruction quantum yield, $\Phi_{295\ nm}$, for the phycobiliproteins is high ($\approx 10^{-3}$, as compared with $\approx 10^{-7}$ for visible light). Energy transfer on a picosecond time scale does not compete with photodestruction. Photodamage to phycobilisomes *in vitro* and in living cells is amplified by causing dissociation and loss of function of the complex. In photosynthetic organisms, UV-B damage to light-harvesting complexes may significantly exceed that to DNA.**

In cells of nonphotosynthetic organisms, DNA absorbs ≈50% of the incident UV-B radiation and is the primary target of photodamage. However, in plants and photosynthetic organisms, chlorophyll and other pigments may contribute significantly to shielding of the DNA from ultraviolet radiation. For example, comparison of absolute action spectra for pyrimidine dimer formation in alfalfa seedlings versus T7 bacteriophage DNA show over a 100-fold decrease in the rate of UV-B-induced DNA damage (1). In cyanobacteria, the most widespread and abundant photosynthetic prokaryotes, we calculate that the light-harvesting proteins (phycobiliproteins and chlorophyll proteins) account for >99% of the UV-B absorption. There are voluminous data on the photochemistry of DNA and on quantum yields of its various photoreactions (e.g., ref. 2). Comparable data on the photodestruction quantum yields of proteins in general and light-harvesting proteins in particular are totally lacking.

To address this deficiency, we present a quantitative study of the photodestruction of the cyanobacterial light-harvesting complex, the phycobilisome (3), by ultraviolet light of 285–305 nm at a photon flux for this 20-nm wavelength band about 50 times that reaching the Earth's surface at the normal stratospheric ozone level of about 300 Dobson units [matm·cm (1 atm = 101.33 kPa)] (4). Cyanobacteria make a dominant contribution to phytoplankton primary productivity. In the range from 285 to 700 nm, phycobilisomes account for over half of the absorption cross-section of cyanobacterial cells. Chlorophyll–protein complexes account for most of the remaining absorbance.

As a test organism, we chose the extensively studied filamentous heterocystous cyanobacterium *Anabaena* strain PCC 7120. A schematic representation of the *Anabaena* phycobilisome is shown in Fig. 1. Allophycocyanin (AP) is the major component of the phycobilisome core (proximal to the reaction centers within the thylakoid membrane), and C-phycocyanin (PC), and phycoerythrocyanin (PEC) are the major and minor components of the rod substructures, respectively. We have studied the photochemistry of the individual phycobiliproteins, of the purified intact as well as dissociated phycobilisomes, and of phycobilisomes in living *Anabaena* cells.

## MATERIALS AND METHODS

***Anabaena* Cells, Phycobilisomes, Phycobiliproteins, and Other Proteins.** *Anabaena* sp. PCC 7120 cells were cultured at 30°C at 17 $\mu$E $m^{-2}$·$sec^{-1}$ [1 E (einstein) = 1 mol of photons] in liquid AA-based medium (6) as modified by Hu *et al.* (7). *Anabaena* sp. PCC 7120 PC, PEC, and AP were prepared by the procedure of Bryant *et al.* (8) with final purification by fast protein liquid chromatography (9). Sperm whale myoglobin and egg-white lysozyme were purchased from Sigma. Spinach ribulosebisphosphate carboxylase was a gift of George H. Lorimer (Dupont).

**HPLC Instrumentation.** HPLC separations were performed as specified below with a Waters model 600E Multisolvent Delivery System equipped with a Waters model 991 Photodiode Array Detector linked to an NEC computer; the computer was used for both gradient control and data acquisition.

**Spectroscopic Measurements.** Absorption spectra were acquired on a computer-controlled dual-beam Perkin–Elmer λ6 UV/Vis spectrophotometer. Excitation spectra were obtained with a Perkin–Elmer model MPF-44B spectrofluorimeter in ratio mode with rhodamine B as a quantum counter. Quartz cuvettes with a 1-cm pathlength were used for absorption and with a 0.4 cm pathlength were used for fluorescence measurements.

**Extinction Coefficients at 295 ± 10 nm for PC and Its α and β Subunits.** Assuming that the three bilins of PC have the same absorbance, $\varepsilon$ at 295 ± 10 nm is 7450 $M^{-1}$·$cm^{-1}$ for the $\alpha$ subunit, 14,900 $M^{-1}$·$cm^{-1}$ for the $\beta$ subunit, and 22,350 $M^{-1}$·$cm^{-1}$ for PC, as calculated from known $\varepsilon_{614\ nm}$ = 279,000 $M^{-1}$·$cm^{-1}$ for PC $\alpha\beta$ (8). The following $\varepsilon_{295\ nm}$ ($M^{-1}$·$cm^{-1}$) values were used for other proteins: AP, 19,500; PEC, 41,900; apomyoglobin, 8,100; ribulosebisphosphate carboxylase, 11,000; lysozyme, 16,500. For tryptophan, $\varepsilon_{295\ nm}$ ($M^{-1}$·$cm^{-1}$) = 2,500.

**Photodestruction Quantum Yield.** The photodestruction quantum yield was calculated as follows: $n(t)/n(0) = \exp(-k_d t)$, where $n(0)$ is the total number of protein molecules at time 0, $n(t)$ is the number of undamaged protein molecules after time $t$ of illumination, and $k_d$ is the photodestruction rate. $k_d = \sigma I \Phi$, where $\sigma$ is the absorption cross-section ($cm^2$) and is related to the molar absorption coefficient $\varepsilon$ ($M^{-1}$·$cm^{-1}$): $\sigma = 3.8 \times 10^{-21}\varepsilon$; $I$ is the illuminating light intensity (photons $sec^{-1}$·$cm^{-2}$); and $\Phi$ is the photodestruction quantum yield (molecules per photon). The data on phycobiliprotein photodestruction was fitted with the equation $n(t)/n(0) = \exp(-\Phi N)$, where $N = 3.8 \times 10^{-21}\varepsilon It$ is the number of photons absorbed per molecule at time t (10). Photodestruction was achieved by illumination with 295 nm (20-nm bandwidth) light from a 150 W xenon arc lamp at a photon flux of 2.6 W $m^{-2}$·(20 nm)$^{-1}$. The average downward global flux at 295 ± 10 nm for an average ozone thickness in the atmosphere of 0.32 cm from a solar zenith angle of 40° is 0.051 W $m^{-2}$·(20 nm)$^{-1}$ (4). This is 51-fold lower than the flux used in these experiments.

**Absorption Cross-Sections for 295 nm Radiation for DNA and Phycobiliproteins in *Anabaena* Cells.** *Anabaena* cells

The publication costs of this article were defrayed in part by page charge payment. This article must therefore be hereby marked "*advertisement*" in accordance with 18 U.S.C. §1734 solely to indicate this fact.

*Abbreviations*: AP, allophycocyanin, PC, C-phycocyanin; PEC, phycoerythrocyanin; PCB, phycocyanobilin.

*To whom reprint requests should be addressed.

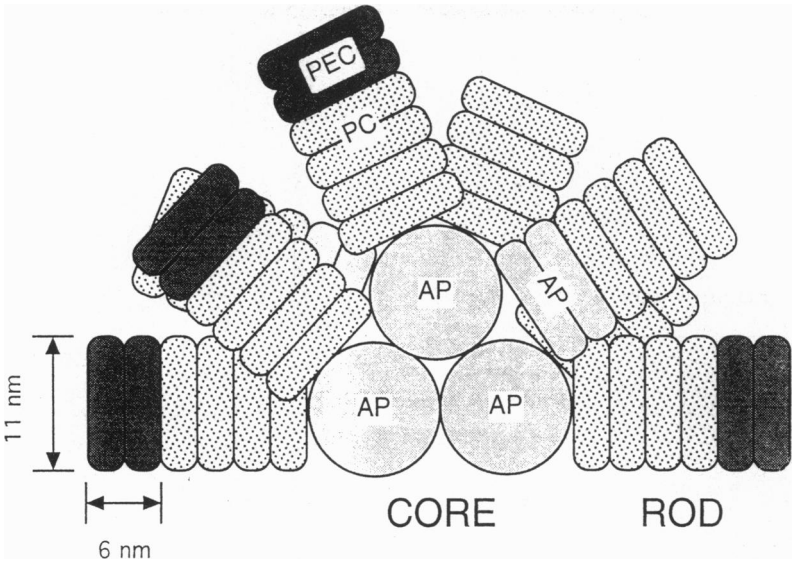


FIG. 1. Schematic representation of the *Anabaena* strain PCC 7120 phycobilisome (5). Each disk in the structure contains a phycobiliprotein trimer $(\alpha\beta)_3$. For abbreviations, see text.

contain ≈0.5% (dry weight) DNA (11) and the phycobiliprotein content of exponentially growing cells is assumed to be about 18% (dry weight) (e.g., ref. 12). The size of the *Anabaena* strain PCC 7120 genome is $6.5 \times 10^6$ base pairs ($3.6 \times 10^{-14}$ g of DNA).

From these data, in an *Anabaena* cell ($7.2 \times 10^{-12}$ g dry weight), there are five copies of the genome and $6.5 \times 10^5$ phycobilisomes (each $7.12 \times 10^6$ Da; based on ref. 5). There are 565 bilins per phycobilisome and a total number of $3.7 \times 10^8$ bilins per cell. The mean $\varepsilon_{295\ nm}$ per base pair is 2,184 $M^{-1}$ $cm^{-1}$ and per bilin is 10,400 $M^{-1}\cdot cm^{-1}$ (this work). Consequently, in an *Anabaena* strain PCC 7120 cell, phycobiliproteins absorb 54 times more 295 nm radiation than the DNA. The photodestruction quantum yield, $\Phi_{295\ nm}$, for thymine dimer formation in bacteriophage T7 DNA is $5 \times 10^{-3}$ (13) and for damage to phycocyanin is $1.9 \times 10^{-3}$ (this work), consequently the ratio of the damage to PC relative to DNA is ≈20.

## RESULTS

**Wavelength Dependence and Quantum Yield of the Photodestruction of *Anabaena* Phycobiliproteins.** Fig. 2*A* shows the absorption spectra of PC recorded after various times of exposure to UV (285–305 nm) illumination. The area under the absorption band from 500–700 nm decreases exponentially as a function of the number of photons absorbed per molecule (Fig. 2*B*). The photodestruction quantum yield of PC ($\Phi_{PC}$), calculated from the absorption decrease, defined as the number of molecules damaged per photon absorbed, is $1.9 \times 10^{-3}$ (see *Materials and Methods*). The values of $\Phi_{PC}$ for visible photons were also determined in this manner and found to be $10^4$ lower ($1.6–2.7 \times 10^{-7}$) (Fig. 2*C*). [White and Stryer (14) reported photodestruction quantum yields at 514.5 nm (based on fluorescence decrease) for PC and AP of $2.5 \times 10^{-6}$ and $4.5 \times 10^{-6}$, respectively.] Thus, UV-B photons are strikingly more effective at damaging phycocyanin than visible photons and are over 100 times more effective than UV-A photons (Fig. 2*C*).

UV (295 ± 10 nm) illumination of native PEC and AP, exactly as described for PC, gave $\Phi_{PEC}$ and $\Phi_{AP}$ values of $2.0 \times 10^{-3}$ and $0.95 \times 10^{-3}$, respectively. The $\Phi_{295\ nm}$ for the free linear tetrapyrrole prosthetic group, phycocyanobilin (PCB), in 8 M urea at pH 2 was $0.71 \times 10^{-3}$.

**Sites of Photodamage.** Does the initial photodamage occur on the protein, on the bilins, or is distributed between the two? PC monomer ($\alpha\beta$) carries three PCBs linked through thioether bonds to cysteinyl residues, $\alpha$-84, $\beta$-82, and $\beta$-155 (3). Analysis of photodamaged PC by SDS/PAGE shows the formation (in low yield) of intersubunit crosslinks and damage to amino acid side chains and bilins, but does not indicate polypeptide backbone cleavage (data not shown). To determine whether there is any selectivity in the photoreactions due to UV-B photons, PC samples irradiated for various lengths of time were analyzed by HPLC on a reverse-phase C-4 column (15). The normalized areas between the half-maxima of the $\alpha$ and $\beta$ subunit peaks (Fig. 3*A*) were plotted as a function of the number of photons absorbed (Fig. 3*B*). Similar results were obtained from plots using data acquired at 280 and 640 nm. The photodestruction quantum yields for the individual subunits ($\alpha$, $2.0 \times 10^{-3}$; $\beta$, $2.6 \times 10^{-3}$) determined from these data are consistent with the value of $1.9 \times 10^{-3}$ determined for the decrease in the absorption spectrum of irradiated native PC (Fig. 2*B*).

$\Phi_{\beta\text{-PC}}$ is 1.3× larger than that for $\alpha$-PC (Fig. 3*B*). A possible explanation for this small difference is that the $\beta$-82 PCB, the terminal energy acceptor in phycocyanin (16–18), receives a higher excitation flux than the other bilins because of energy transfer and is damaged preferentially. This explanation was tested in two ways. UV-B-irradiated PC samples were digested with trypsin, the tryptic peptides were separated on a C-18 column, and the damage to the individual bilins was assessed. The rate of damage to the bilins at $\beta$-82 and $\beta$-155 was found to be equal (data not shown). In an independent set of experiments, PC was denatured in 8 M urea at pH 2, and then irradiated in the same manner as the native PC. HPLC analysis under the conditions specified for Fig. 3*A* gave results quantitatively the same as those obtained for the native protein. Consequently, there is no detectable effect of energy transfer or of native protein structure on the relative rates of photodestruction of particular PCBs.

**UV (295 ± 10 nm) Damage to Other Proteins.** Experiments on several unrelated proteins, lacking prosthetic groups, gave similar $\Phi_{295\ nm}$ values, reflective of damage to the aromatic amino acids. For example, the $\Phi_{295\ nm}$ values determined for apomyoglobin, lysozyme, and ribulosebisphosphate carboxylase were $3.9 \times 10^{-3}$, $6.0 \times 10^{-3}$, and $5.0 \times 10^{-3}$, respectively (determined by monitoring loss of tryptophan fluorescence; data not shown). The $\Phi_{295\ nm}$ values determined by HPLC for apomyoglobin, lysozyme, and ribulosebisphosphate carboxylase small subunit were $2.9 \times 10^{-3}$, $1.3 \times 10^{-3}$, and $6.7 \times 10^{-3}$, respectively (data not shown).

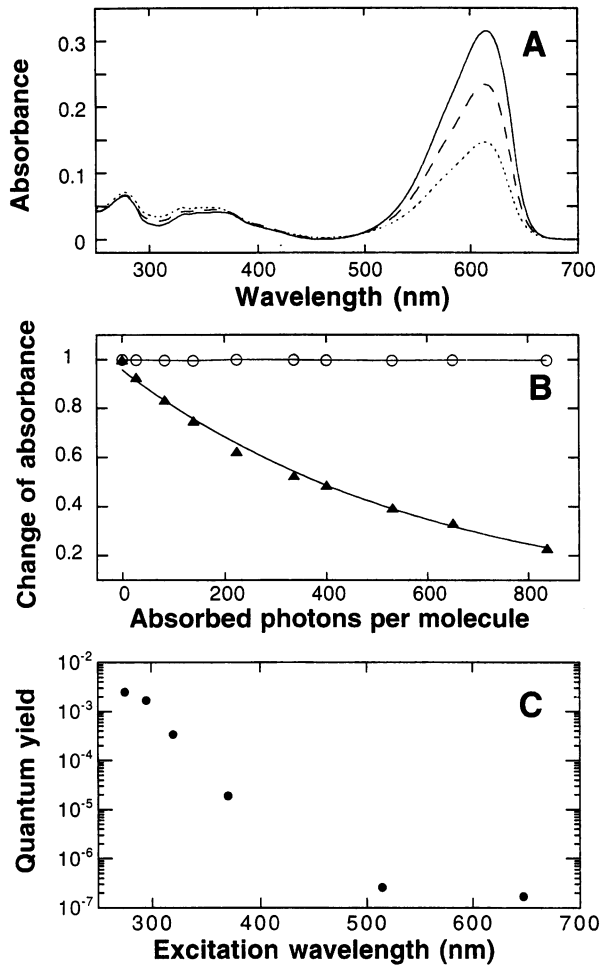


FIG. 2. (*A*) Absorption spectra of PC ($\varepsilon_{295\ nm}$ 22,346 $M^{-1}\cdot cm^{-1}$ per PC $\alpha\beta$ monomer) in 100 mM sodium phosphate buffer, pH 8.0, taken at time zero, and after 150 min (---) and 430 min (. . . .) of illumination with 295 nm (20 nm bandwidth) light from a 150 W xenon arc lamp at a photon flux of 2.6 W $m^{-2}\cdot(20\ nm)^{-1}$. (*B*) Change in absorption of PC as a function of the number of photons absorbed per molecule (▲). The data were fitted with a single exponential decay curve yielding a $\Phi_{PC}$ of $1.9 \pm 0.3 \times 10^{-3}$ (triplicate). Absorption spectra of a control sample kept in the dark are indicated by circles. (*C*) Wavelength dependence of $\Phi_{PC}$. The extinction coefficients are per PC $\alpha\beta$ monomer. $\Phi_{PC}$ (275 nm) = $2.5 \times 10^{-3}$ at a flux of 2.2 W $m^{-2}\cdot(20\ nm)^{-1}$ ($\varepsilon_{275\ nm}$ 55,545 $M^{-1}\cdot cm^{-1}$); $\Phi_{PC}$ (370 nm; 20 nm bandpass) = $1.9 \times 10^{-5}$ at a flux of 8.8 W $m^{-2}\cdot(20\ nm)^{-1}$ ($\varepsilon_{370\ nm}$ 39,900 $M^{-1}\cdot cm^{-1}$); $\Phi_{PC}$ (514 nm; argon ion laser) = $2.6 \times 10^{-7}$ at a flux of 27 W $cm^{-2}$ ($\varepsilon_{514\ nm}$ 23,300 $M^{-1}\cdot cm^{-1}$); $\Phi_{PC}$ (647 nm; krypton ion laser) = $1.7 \times 10^{-7}$ at a flux of 4.5 W $cm^{-2}$ ($\varepsilon_{647\ nm}$ 57,940 $M^{-1}\cdot cm^{-1}$).

**Photodestruction of Phycobiliproteins in Intact Phycobilisomes.** Intuitively, one might expect that the availability of rapid radiationless energy transfer pathways might protect the groups initially excited from photodestruction. The phycobilisome offers an excellent test object for the exploration of such expectation. Transfer of energy from proteins in the phycobilisome rods (PEC and PC) to the core proceeds in 100 ps or less with an overall efficiency >95% (19). The absorption spectra of phycobilisomes AP, PC, and PEC are virtually the same as their fluorescence excitation spectra, between 250 and 600 nm, showing that the energy transfer for UV-B excitation is as efficient as that for visible light.

We next examined the photodestruction of phycobilisomes. UV-B irradiation of phycobilisomes leads to rapid decrease in the 680-nm fluorescence emission from the terminal energy acceptor bilins in the core (Fig. 4*A*); a 60% decrease is seen in 30 min (Fig. 4*B*, solid line). The 640 nm fluorescence emitted

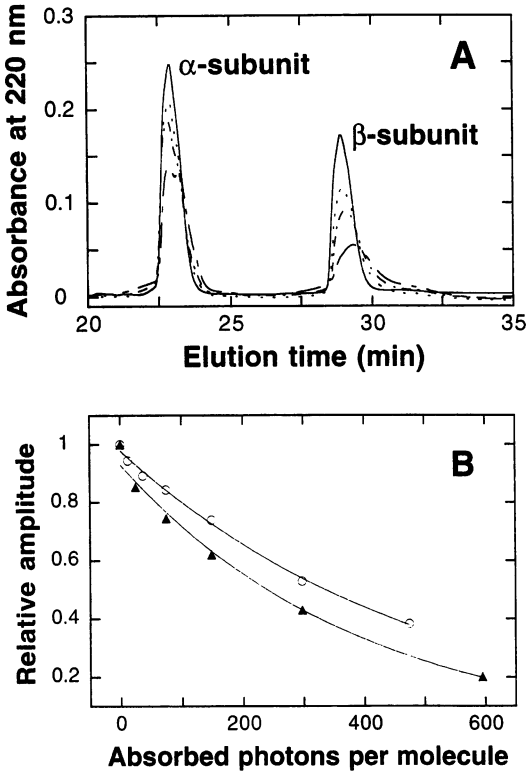


FIG. 3. Determination of the photodestruction quantum yields for the PC $\alpha$ and $\beta$ subunits. (*A*) HPLC profiles of PC exposed to increasing lengths of time (0, 138, 318, 765 min) to 295 nm illumination. PC samples (200 μl, initial $A_{620\ nm}$ = 1.0) were injected onto a C-4 reverse-phase column preequilibrated with 65% 0.1:99.9 (vol/vol) trifluoroacetic acid/water. 35% 2:1 (vol/vol) acetonitrile/isopropanol. Elution was performed according to ref. 15 at a flow rate of 1.5 $ml\cdot min^{-1}$. Only the data for time interval from 20 to 35 min are shown. No peaks were detected outside of this time range. (*B*) The integrated areas between the half-maxima for the $\alpha$ subunit (○) and the $\beta$ subunit (▲) peaks are plotted as a function of the photons absorbed per molecule. The solid lines are single exponential fits with $\Phi_{\alpha\text{-}PC} = 2.0 \times 10^{-3}$ and $\Phi_{\beta\text{-}PC} = 2.6 \times 10^{-3}$.

by the rod phycobiliproteins follows a more complex time course (Fig. 4*B*, dotted line). An initial fast decrease is followed by an increase in fluorescence, and then followed by a slower decrease. The wavelength dependence of the photodestruction quantum yield at 20°C for phycocyanin (Fig. 2*C*) and for phycobilisomes (Fig. 4*C*) is very similar indicating that thermal effects are not contributing to phycobilisome disassembly.

Comparing the decay curves at 640 and 680 nm, the following reasons (singly or in combination) might be suggested for the fast decay of the fluorescence from the core: (*i*) the excitation energy absorbed by the proteins in the rods is funneled to the core, thus damaging the proteins in the core and protecting those in the rods; (*ii*) the energy transfer pathways within the phycobilisome are disrupted because of dissociation of the complex; and (*iii*) the energy transfer efficiency within the phycobilisome is much decreased due to photodamage without physical disruption of the complex.

We have evaluated these possibilities by examining the distribution of photodamage between PC and AP in irradiated phycobilisomes. The HPLC profile of phycobiliprotein subunits was monitored at 640 nm. At this wavelength, the PEC $\alpha$ subunit does not absorb. PC $\beta$, PEC $\beta$, and AP $\alpha$ subunits all elute together at 29 min, but PC $\alpha$ at 23 min and AP $\beta$ at 32 min are each well resolved from other components. From Fig. 5 *A* and *B*, it is seen that in phycobilisomes the damage to PC (in the rods) and AP (in the core) is very similar to that seen for the individual purified phycobiliproteins. Moreover, the

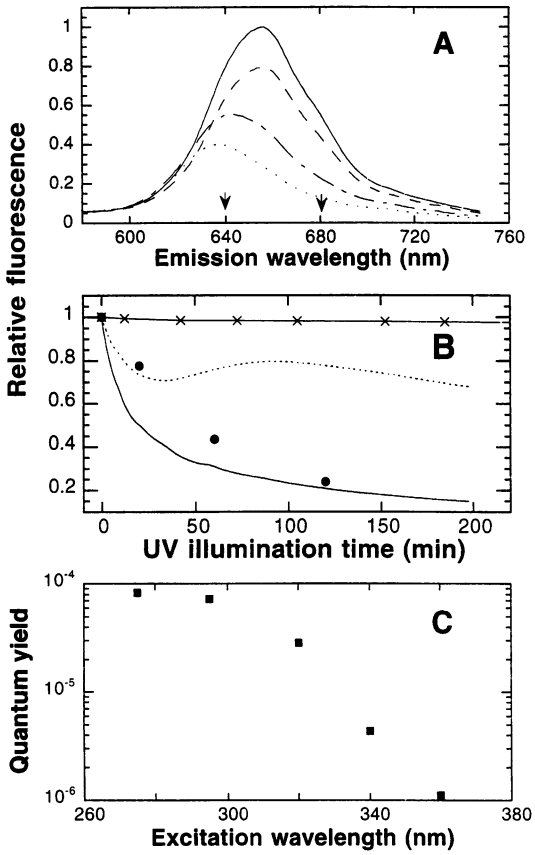


FIG. 4. (*A*) The complete phycobilisome emission spectra for excitation at 295 nm after UV-B illumination for 0, 10, 50, and 130 min. Arrows indicate wavelengths (640 nm and 680 nm) monitored continuously during illumination. (*B*) Effect of UV-B illumination ($\lambda_{exc}$ 295 nm) on the fluorescence emission at 680 nm from the core (solid line) and at 640 nm from the rods (dashed line) of *Anabaena* phycobilisomes ($A_{620\ nm}$ = 0.07) in 0.7 M sodium/potassium phosphate buffer, pH 8. ●, Residual fraction of intact phycobilisomes at each time point (0, 20, 60, and 120 min at 295 nm illumination) as determined after sucrose density gradient centrifugation (20); ×, the 680 nm fluorescence of a control phycobilisome sample kept in the dark and probed at intervals with 560 nm excitation. (*C*) Dependence of the photodestruction quantum yield of phycobilisomes (determined from the fractional decrease in 680 nm fluorescence) on excitation wavelength in the UV-B/UV-A region.

pattern of UV-B-induced damage is the same for intact phycobilisomes in high salt buffer (700 mM sodium/potassium phosphate, pH 8), and for completely dissociated phycobilisomes in low salt buffer (10 mM NaK-phosphate, pH 8) (Fig. 5 *A–C*). These results show that rapid energy transfer from PC to AP within the phycobilisome does not affect the rate of bilin destruction in PC.

The HPLC data (Fig. 5 *A* and *B*) show that the damage to PC and AP in intact phycobilisomes after 60 min of UV illumination is 20–30%, whereas the fluorescence from the core decreases by almost 80% (see Fig. 4*B*). Thus, the loss of energy transfer in irradiated phycobilisomes is far more extensive than the damage to phycobiliproteins. The dissociation of phycobilisomes as a function of UV-B illumination was quantitated by sucrose density gradient centrifugation (ref. 20; see Fig. 4*B*, solid circles). The results show that the time-course of the loss of intact phycobilisomes correlates closely with the decrease in 680 nm fluorescence. Consequently, the damage to the individual phycobilisome components is amplified by the resulting dissociation of this macromolecular complex. The above results show decisively that energy transfer processes within individual phycobiliproteins or phycobilisomes do not affect the pattern of UV-B photodamage.

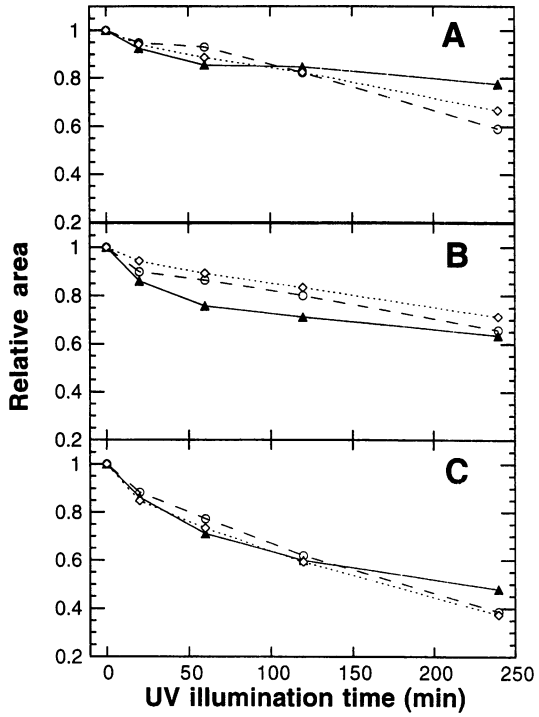


FIG. 5. Photodestruction rate of phycobiliprotein subunits in intact and dissociated phycobilisomes and in purified phycobiliproteins illuminated at 295 nm for up to 240 min. Phycobiliprotein polypeptides (200 μl, initial $A_{650\ nm}$ = 1.0) were separated by HPLC as described in Fig. 3 and absorbance was monitored at 640 nm. For each peak, areas were integrated between the half-maxima. The samples were as follows: phycobilisomes in 0.7 M sodium/potassium phosphate (pH 8), dissociated phycobilisomes in 10 mM sodium/potassium phosphate (pH 8), and purified phycobiliprotein in 100 mM sodium/potassium phosphate buffer (pH 8). (*A*) AP β subunit in intact (▲) and dissociated (○) phycobilisomes and in pure AP (◇). (*B*) PC α subunit in intact (▲) and dissociated (○) phycobilisomes, and in pure PC (◇). (*C*) The sum of the PC β, AP α, and PEC β subunits in intact (▲) and dissociated (○) phycobilisomes, and of PC β in pure PC (◇).

**Photodestruction of Phycobilisomes in Living Cells.** The UV (295 ± 10 nm) photon flux used here is about 50-fold stronger than the average UV-B radiation of sunlight (4). Our results show that energy transfer from purified phycobilisomes will be decreased by some 60% by exposure to the UV-B in sunlight in 17 h (Fig. 4*B*). Such a destruction rate is significant relative to the doubling time of *Anabaena* strain PCC 7120 of about 12 h. The rate of phycobilisome damage in living cells might be significantly slower, because cyanobacteria commonly possess "sunscreen" compounds (e.g., ref. 21). To determine the rate of UV-B damage *in vivo*, dilute cell suspensions were illuminated with 295 nm light. Damage was assessed by periodically probing the cells with 560 nm light, where only the phycobilisome absorbs, and following the decrease in the 680-nm fluorescence emission from the terminal energy acceptors in the phycobilisome core. This experiment assumes that energy transfer to reaction centers does not reduce photodamage to phycobilisomes, and that fluorescence emitted from the phycobilisome core is insensitive to UV-B damage of reaction centers. The ratio of the rates of decay of 680 nm fluorescence for purified phycobilisomes versus phycobilisomes in intact cells was determined to be 0.6 ± 0.1 (Fig. 6). Consequently, the sunscreen factor for *Anabaena* strain PCC 7120 is 0.4. This compares well to shielding factors at 320 nm of 0.2–0.6 estimated for a wide variety of UV-B-adapted cyanobacterial strains by quantitation of cell content of shielding compounds (mycosporine amino acid-like compounds and scytonemin) (21).

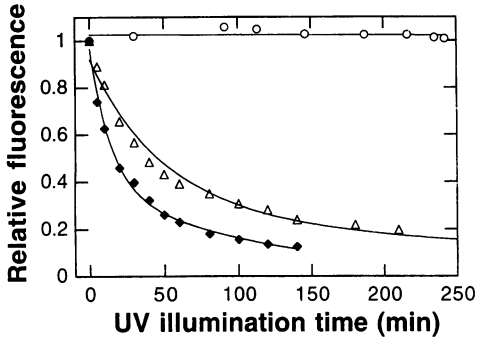


FIG. 6. Comparison of the rate of photodestruction of purified phycobilisomes and of phycobilisomes in whole *Anabaena* cells. Phycobilisome damage was monitored as a function of time of 295 nm irradiation by excitation at 560 nm (where only the phycobilisome has significant absorbance) and measurement of fluorescence emission at 680 nm. Cells (apparent $A_{295\ nm} = 0.05$) in culture medium (see text) containing 10% (wt/vol) dextran sulfate to prevent settling, were either kept in the dark (○) or illuminated at 295 nm (△). Phycobilisomes were in 0.7 M sodium/potassium phosphate, pH 8. The phycobilisome data (◆) were fitted with double-exponential functions. The whole cell data were fitted with the same double-exponential functions incorporating an additional parameter ($\eta$) to account for the "sunscreen" factor (see text) in the exponents. A correction was applied to compensate for the contribution to absorption and scatter of the 10% dextran sulfate (apparent $A_{295\ nm} = 0.16$). A value of $\eta$ of 0.6 ± 0.1 gave optimum fit to the whole cell data indicating a sunscreen factor of 0.4.

Consistent with the above observations, Sinha *et al.* (22) have shown that irradiation of living cells of *Anabaena* sp. or *Nostoc carmium* with broad band (280–400 nm) UV light leads to time-dependent phycobiliprotein destruction and phycobilisome disassembly.

## DISCUSSION

The photodestruction quantum yield, $\Phi_{295\ nm}$, for the phycobiliproteins, whether denatured, native, or within phycobilisomes is $\approx 10^{-3}$. Experiments on several unrelated proteins, lacking prosthetic groups, gave similar $\Phi_{295\ nm}$ values, reflective of damage to the aromatic amino acids. For example, the $\Phi_{295\ nm}$ values determined for apomyoglobin, lysozyme, and ribulosebisphosphate carboxylase were $3.9 \times 10^{-3}$, $6.0 \times 10^{-3}$, and $5.0 \times 10^{-3}$, respectively (determined by monitoring loss of tryptophan fluorescence; with similar $\Phi_{295\ nm}$ values determined by HPLC). Moreover, published $\Phi_{313\ nm}$ values (given in parentheses; ref. 23) for diverse aromatic compounds fall into this range, for example, napthalene ($1.5 \times 10^{-2}$), anthracene ($3.0 \times 10^{-3}$), 2,4-dinitrotoluene ($2.0 \times 10^{-3}$), and tryptophan ($1.4 \times 10^{-2}$; this study). From the similarity in these photodestruction quantum yields to that of free bilin, we conclude that the initial photodamage in the phycobiliproteins is the sum of the direct damage to the aromatic amino acids in the protein moiety and direct damage to the bilins, with the relative proportion determined by their absorption cross sections and photodestruction quantum yields. The reactive species generated by photodamage then undergo a variety of secondary chemical reactions. In summary, phycobiliproteins in cyanobacterial cells will be destroyed faster by 295 ± 10 nm radiation than proteins that do not bear light-absorbing prosthetic groups simply because their absorption cross-section is increased by the contributions of their bilins and because they are the most abundant proteins in the cell.

The results we have presented decisively support the surprising conclusion that energy transfer processes within individual phycobiliproteins or phycobilisomes do not affect the pattern of UV-B photodamage. The energies of UV-B photons (<320 nm) are above the threshold for the breakage of certain covalent bonds. Because fast intramolecular energy transfer processes (*ca.* 10 ps) do not protect particular bilins from damage, the photodamage processes must occur on a <100 fs time scale. For a given chromophore, the photodestruction quantum yield is governed by the nonstationary vibrational state distribution of the molecules on the excited state surface (24). We have not explored possible contributions to the photodestruction through mechanisms dependent on oxygen activation by either singlet or triplet states of chromophores. However, White and Stryer (14) showed that the rate of phycobiliprotein photodestruction by 514.5 nm light was unchanged when the $O_2$ concentration was reduced 20-fold by flushing with argon.

Consideration of absorption cross-sections and photodestruction quantum yields for UV-B photons of purified phycobiliproteins and of DNA shows that phycobiliproteins will be destroyed about 20-times faster than DNA bases (see calculation in *Materials and Methods*). This is a gross underestimate of the ratio of the relative net destruction rates *in vivo*, because in living cells, shielding, effective repair reactions, and the presence of multiple copies of the genome, all mitigate photodamage to DNA. Replacement of photodamaged phycobiliproteins requires breakdown and resynthesis of the damaged molecules. Our studies provide no information on the rate of these processes in living cells exposed to the full solar spectrum.

Earlier qualitative studies of other photosynthetic systems (e.g., refs. 25–27) led to the conclusion that solar flux UV-B-induced damage *in vivo* to the photosynthetic light-harvesting pigments in various photosynthetic organisms and higher plants is significant and has an effect on their photosynthetic capacity and consequently on primary productivity.

The flux of solar ultraviolet radiation of 280–320 nm (UV-B) at the Earth's surface is strongly dependent on the concentration of stratospheric ozone. The average total ozone in the atmosphere is equivalent to about 300 Dobson units (matm·cm), but decreases to half of this amount have been measured under the Antarctic ozone "hole" (e.g., ref. 28). The impact of this decrease is almost exclusively on the transmittance of the UV-B portion of solar radiation. The average downward global flux at 295 ± 10 nm for a reduced average ozone thickness in the atmosphere of 0.16 cm from a solar zenith angle of 40° is 0.24 W $m^{-2}$·$(20\ nm)^{-1}$ (4). This is only 11-fold lower than the flux [2.6 W $m^{-2}$·$(20\ nm)^{-1}$] used in the experiments reported here and would be anticipated to damage some 60% of the phycobilisomes in living cells in 6–7 h, if living cells were located at the air/earth interface.

It is believed that many species of phytoplankton in marine ecosystems are sensitive to UV-B, even at low doses. In the absence of an $O_3$ hole, ambient levels of springtime UV-B radiation are reported to suppress daily rates of Antarctic primary production by some 4–7% in surface waters (2 m). A 50% $O_3$ depletion is claimed to bring about an additional 5–16% decrease in rates of primary production in the upper part of the water column (29).

There has been no assay, independent of global measurements of photosynthesis, that would provide direct information on structural damage to the cyanobacterial photosynthetic apparatus under various conditions encountered in the field. In earlier studies, we have shown that time-resolved measurements of fluorescence emission of living marine unicellular cyanobacteria serve as a highly sensitive and quantitative guide to the structural integrity of their phycobilisomes (30). The results we present here suggest that careful study of the fluorescence properties of cyanobacteria subjected to various levels of UV-B photon flux may reveal distinctive spectroscopic signatures that can be used to analyze rapidly single cells in the field to detect and quantitate damage to phycobilisomes. In this manner, one would be able to assay objectively, for at least one class of photosynthetic organisms that occupy virtu-

ally every ecological niche, the effect of the recorded variation in the solar UV-B flux on the photosynthetic apparatus.

We thank R. A. Mathies for a critical reading of this manuscript and H. C. M. Nelson for helpful comments. Supported in part by grants from the National Institute of General Medical Sciences (GM28994) and the Lucille P. Markey Charitable Trust.

1. Quaite, F. E., Sutherland, B. M. & Sutherland, J. C. (1992) *Nature (London)* **358,** 576–578.
2. Görtner, H. (1994) *J. Photochem. Photobiol. B Biol.* **26,** 117–139.
3. Glazer, A. N. (1989) *J. Biol. Chem.* **264,** 1–4.
4. Shettle, E. P., Nack, M. L. & Green, A. E. S. (1975) in *Impacts of Climatic Change on the Biosphere,* eds. Nachwey, D. S., Caldwell, M. M. & Biggs, R. H. (Natl. Tech. Inform. Serv., Springfield, VA), Vol. 1, pp. 2.38–2.49.
5. Glauser, M., Bryant, D. A., Frank, G., Wehrli, E., Sidler, W. & Zuber, H. (1992) *Eur. J. Biochem.* **205,** 907–915.
6. Allen, M. B. & Arnon, D. I. (1955) *Plant Physiol.* **30,** 363–372.
7. Hu, N.-T., Thiel, T., Giddings, T. H. & Wolk, C. P. (1982) *Virology* **114,** 236–246.
8. Bryant, D. A., Glazer, A. N. & Eiserling, F. A. (1976) *Arch. Microbiol.* **110,** 61–75.
9. Swanson, R. V. & Glazer, A. N. (1990) *J. Mol. Biol.* **214,** 787–796.
10. Mathies, R. A. & Stryer, L. (1986) in *Applications of Fluorescence in the Biomedical Sciences,* eds. Taylor, D. L., Waggoner, A. S., Murphy, R. F., Lanni, F. & Birge, R. (Liss, New York), pp. 129–140.
11. Carr, I. W., Leach, C. K. & Carr, N. G. (1969) *Arch. Mikrobiol.* **65,** 218–227.
12. Bennett, A. & Bogorad, L. (1973) *J. Cell Biol.* **58,** 419–435.
13. Emrick, A. & Sutherland, J. C. (1989) *Photochem. Photobiol.* **49,** 35S.
14. White, J. C. & Stryer, L. (1987) *Anal. Biochem.* **161,** 442–452.
15. Swanson, R. V. & Glazer, A. N. (1990) *Anal. Biochem.* **188,** 295–299.
16. Siebzehnrübl, S., Fischer, R. & Scheer, H. (1987) *Z. Naturforsch. Sect. C Biosci.* **42,** 258–262.
17. Schirmer, T. & Vincent, M. G. (1987) *Biochim. Biophys. Acta* **893,** 379–385.
18. Ong, L. J. & Glazer, A. N. (1991) *J. Biol. Chem.* **266,** 9515–9527.
19. Glazer, A. N., Yeh, S. W., Webb, S. P. & Clark, J. H. (1985) *Science* **227,** 419–423.
20. Glazer, A. N. (1988) *Methods Enzymol.* **167,** 291–303.
21. Garcia-Pichel, F. & Castenholz, R. W. (1993) *Appl. Env. Microbiol.* **59,** 163–169.
22. Sinha, R. P., Liebert, M., Kumar, A., Kumar, H. D. & Häder, D.-P. (1995) *Bot. Acta* **108,** 87–92.
23. Schwarzenbach, R. P., Gschwend, P. M. & Imboden, D. M. (1993) *Environmental Organic Chemistry* (Wiley, New York), p. 470.
24. Wang, Q., Schoenlein, R. W., Peteanu, L. A., Mathies, R. A. & Shank, C. V. (1994) *Science* **266,** 422–424.
25. Helbling, W., Villafane, V., Ferrario, M. & Holm-Hansen, O. (1992) *Mar. Ecol. Prog. Ser.* **80,** 89–100.
26. Gerber, S. & Häder, D.-P. (1992) *Biochem. Syst. Ecol.* **20,** 485–492.
27. Teramura, A. H. & Sullivan, J. H. (1994) *Photosynth. Res.* **39,** 463–473.
28. Stolarski, R. S., Bojkov, R., Bishop, L., Zerefos, C., Staehelin, J. & Zawondny, J. (1992) *Science* **256,** 342–349.
29. Prézelin, B. B., Boucher, N. P. & Schofield, O. (1994) *Stratospheric Ozone Depletion/UV-B Radiation in the Biosphere,* eds. Biggs, R. H. & Joyner, M. E. B. (Springer, Berlin), pp. 181–194.
30. Yeh, S. W., Ong, L. J. & Glazer, A. N. (1986) *Science* **234,** 1422–1424.